

52nd Hatfield Memorial Lecture

Large chunks of very strong steel

H. K. D. H. Bhadeshia*

Most new materials are introduced by selectively comparing their properties against those of steels. Steels set this standard because iron and its alloys have so much potential that new concepts are discovered and implemented with notorious regularity. In this 52nd Hatfield Memorial Lecture, I describe a remarkably beautiful microstructure consisting of slender crystals of ferrite, whose controlling scale compares well with that of carbon nanotubes. The crystals are generated by the partial transformation of austenite, resulting in an extraordinary combination of strength, hardness and toughness. All this is in bulk steel without the use of expensive alloying elements. We now have a strong alloy of iron, which can be used for making items that are large in all three dimensions, which can be made without the need for mechanical processing or rapid cooling and is cheap to produce and apply.

Keywords: Nanotubes, Strong steel, Bainite, Space elevator, Entropy defects

Introduction

It is possible to think of many ways of creating extremely strong materials. Polycrystalline metals can be strengthened by reducing the scale of the microstructure whereas single crystals benefit from perfection. Carbon based materials can in principle become incredibly strong if the only mode of deformation involves stretching of carbon-carbon covalent bonds. These and many other mechanisms of strengthening unfortunately have limitations. In particular, it is difficult to make strong, isotropic materials which can be used to manufacture large components of arbitrary shape, while maintaining an attractive combination of properties at a reasonable cost. Such a material would be commercially viable over a broad range of applications.

Imagine in this context, an exceedingly strong steel that can be made in large chunks, one that is easy to manufacture and has an affordable cost. Before describing this novel material, it is important to review the meaning of strength because there are many promises in the modern scientific and popular literature of materials which possess strength beyond our dreams. I shall attempt in this lecture to make appropriate comparisons to show how steels feature in this scenario.

Theoretical strength

The strength of crystals increases sharply as they are made smaller.¹⁻⁷ This is because the chances of avoiding defects become greater as the volume of the specimen decreases. In the case of metals, imperfections in the form of dislocations are able to facilitate shearing at

much lower stresses than would be the case if whole planes of atoms had to collectively slide across each other.^{8,9} Because defects are very difficult to avoid, the strength in the absence of defects is said to be that of an *ideal* crystal.

In an ideal crystal, the tensile strength is $\sigma_t \approx 0.1E$, where E is the Young's modulus. The corresponding ideal shear strength is $\sigma_s \approx b\mu/2\pi a$, where μ is the shear modulus, b a repeat period along the displacement direction and a the spacing of the slip planes.⁸ For ferritic iron, $\mu=80.65$ GPa and $E \approx 208.2$ GPa.¹⁰ It follows that the ideal values of tensile and shear strength should be ~ 21 and ~ 11 GPa, respectively. In fact, tensile strengths approaching the theoretical values were achieved by Brenner as long ago as 1956 during testing whiskers of iron of $<2 \mu\text{m}$ diameter (Fig. 1a).^{5,7} It is interesting that these stress levels fall out of the regime where Hooke's law applies (Fig. 1b).

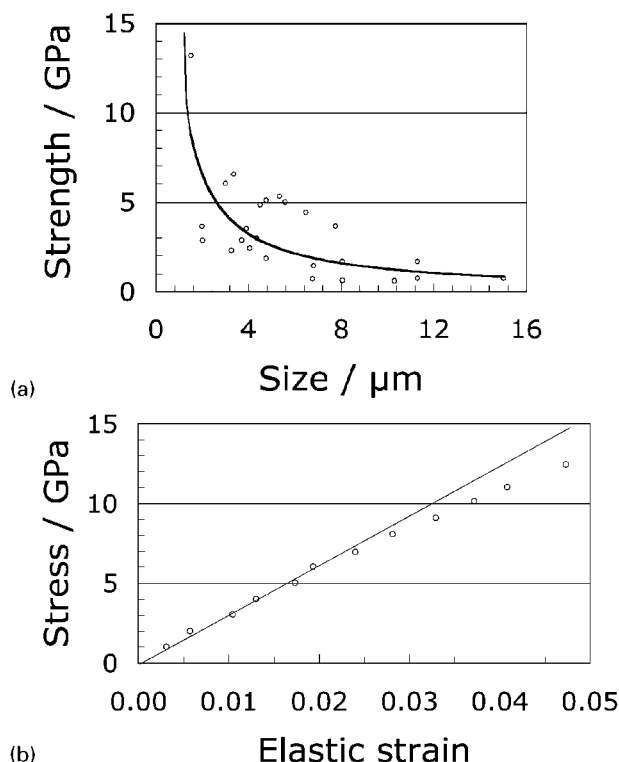
The strength decreased sharply as the dimensions of the whiskers increased (Fig. 1a), because of 'defects which are distributed statistically in a rather complex manner'.^{5,7} Therefore, it was recognised many decades ago that it is not wise to rely on perfection as a method of designing strong materials, although it remains the case that incredible strength can be achieved by reducing dimensions, in the case of iron, to a micrometre scale. It is in this context that we now proceed to examine claims that large scale engineering structures can be designed using long carbon nanotubes.^{11,12}

Gigatubes

The existence of single walled carbon tubes was pointed out in 1976,¹³ but the subject seems to have become prominent after the discovery of C_{60} in 1985¹⁴ and the identification of nanotubes by Iijima in 1991.¹⁵ These tubes can be imagined to be constructed from sheets of

Department of Materials Science and Metallurgy, University of Cambridge, Pembroke Street, Cambridge CB2 3QZ, UK

*Corresponding author, email hkdb@cus.cam.ac.uk



1 a Tensile strength of iron whiskers and b non-linear elasticity at large stresses^{5,7}

graphene consisting of sp^2 carbon arranged in a two dimensional hexagonal lattice (Fig. 2).¹⁶ The sheets, when rolled up and with the butting edges appropriately bonded, are the nanotubes, which may be capped by fullerene hemispheres or not. This is a simplified picture: it is well known that the actual form can be complex, for example with occasional pentagonal rings of carbon atoms instead of hexagonal rings to accommodate changes in shape.¹⁷

The carbon-carbon chemical bond in a graphene layer may be the strongest bond in an extended system;¹⁸ carbon is also light, therefore it is not surprising that there are numerous papers with respect to the potential of long carbon nanotubes as engineering materials which rival steel. The modulus of these tubes along the axis is $\sim 1.28 \pm 0.59$ TPa,¹⁸ comparable with that of diamond.¹⁹

The calculated breaking strength of such a tube has been estimated to be 130 GPa;²⁰ this number is so astonishing that it has led to many exaggerated statements that are frequently repeated and therefore have taken the form of 'truth' in the published literature. For example, the tubes are said to be a hundred times stronger than steel; we have seen that iron whiskers that are much bigger than carbon nanotubes, achieve a strength of 14 GPa with the potential of reaching 21 GPa.

In the literature, there are bizarre statements which take no account of defects. For example, it is said that a 'macroscopic 1 in. thick rope, where 1014 parallel buckywires (nanotube ropes) are all holding together', will be as strong as theory predicts, i.e. 130 GPa.²¹

What all of this ignores is that materials will contain defects.* Some of these defects will be there at

*The author does not mean conformal defects such as the Stone-Wales configurations which become stable and mobile under stress.²² Rather, the author refers to defects which are in principle stable in a stress-free tube and remain so under the influence of load.

equilibrium, i.e. they cannot be avoided. For example, it is known that metals contain an equilibrium concentration of vacancies. The enthalpy change associated with the formation of a vacancy opposes its existence, whereas the change in configurational entropy owing to the formation of a vacancy favours its formation. The total change in free energy on forming n vacancies in a crystal is given by²³

$$\Delta G = n\Delta g - kT[(N+n)\ln(N+n) - N\ln(N) - n\ln(n)] \quad (1)$$

where k is the Boltzmann constant, T the absolute temperature, N the number of atoms. $\Delta g = \Delta h - T\Delta s$, where Δh is the formation enthalpy of one vacancy and Δs the formation entropy of a vacancy excluding any contribution from configurational entropy, which is the second term in equation (1). The equilibrium mole fraction of vacancies x is obtained by writing $\partial\Delta G/\partial n = 0$

$$x = n/N \approx \exp(-\Delta g/kT) \quad (2)$$

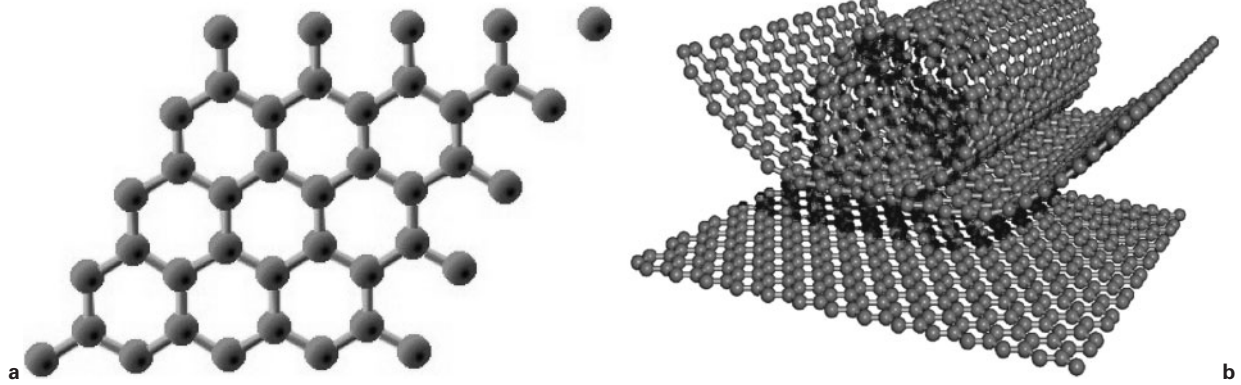
Edwards has estimated that 120 000 km gigatubes grown with the properties of carbon nanotubes are needed to construct a space elevator.¹¹ He further estimates that such a cable would weigh ~ 5000 kg. Based on this, assuming an upper limit of $\Delta g \approx 7$ eV (Ref. 20) and neglecting dimensionality differences, equation (2) can be used to calculate the equilibrium number of monovacancies expected as a function of temperature (Fig. 3). In this, the temperature of interest is that at which the carbon is assembled; this can typically range from 2000 to 4000 K, giving a large number of equilibrium defects. Given that the actual value of Δg is much smaller than the 7 eV for a flat graphene sheet,²⁰ it cannot ever be assumed that defect free gigatubes can be made with properties approaching tubes which are some 18 orders of magnitude smaller.

Statement 1: systems which rely on perfection in order to achieve strength necessarily fail on scaling to engineering dimensions. Indeed, there is no carbon tube which can match the strength of iron beyond a scale of 2 mm.

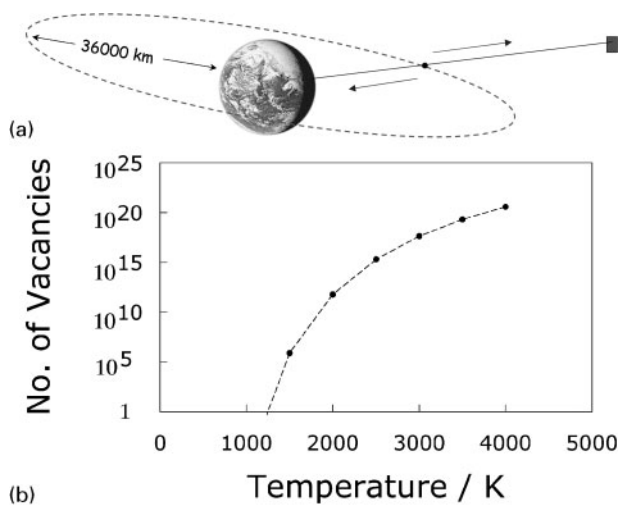
Although vacancies have been considered here and many assumptions have been made in the estimation of defect density, the fact that the measured strengths of nanotubes as shown in Table 1 are frequently much smaller than expected from vacancy models²⁴ indicates the presence of more severe defects in the atomic structure of the tubes. In Table 1, the calculation of strength is based on the cross-sectional area of the nanotube shell rather than the actual cross-sectional area as is normal practice. In the latter case, the strength of short nanotubes decreases by ~ 1 order of magnitude.²⁶ The data also neglect interactions between nesting tubes in the multiwalled nanotubes studied.

Fracture of gigatubes

Suppose that carbon gigatubes could be made capable of supporting a stress of 130 GPa. Would this allow safe engineering design? One aspect of safe design is that fast fracture should be avoided; most metals absorb energy in the form of plastic deformation before ultimate fracture. Energy absorption in an accident is a key aspect of automobile safety. In this sense, carbon nanotubes are not defect tolerant; their deformation



2 a Graphene sheet and b schematic diagram showing how graphene sheet might be rolled to form tube¹⁶



3 a Space elevator concept (originally owing to Arthur C. Clark), requiring cable 120 000 km in length.¹¹ Cable would be launched in both directions from geosynchronous orbit at height of 36 000 km. b Calculated number of single atom vacancies in 5000 kg of carbon nanotubes

before fracture is elastic. The stored energy density in a tube stressed to 130 GPa, and given an elastic modulus along its length of $E=1.2$ TPa is in excess of that associated with dynamite (Table 2). Dynamite is explosive because of its high energy density and because this energy is released rapidly, the detonation front propagating at ~ 6000 m s⁻¹. The speed of an elastic wave in the carbon is given by $(E/\rho)^{1/2}$, where ρ is the density. In the event of fracture, the rate at which the stored energy

Table 1 Measured strength of carbon nanotube based ropes as function of length

Length	Strength, GPa	Reference
460 nm	150	25
1.8 μ m	24	26
2.9 μ m	28	26
6.0 μ m	39	26
6.5 μ m	20	26
6.7 μ m	35	26
6.9 μ m	63	26
11.0 μ m	21	26
1–2 mm	3.6	27
2 mm	1.7	28

would be released is much greater than that of dynamite, meaning that fracture is unlikely to occur in a safe manner (Table 2).

Statement 2: structures in tension, which reversibly store energy far in excess of their ability to do work during fracture, must be regarded as unsafe.

Strengthening by deformation

For some time, it has been possible to commercially obtain steel wire which has an ultimate tensile strength of 5.5 GPa and yet is very ductile in fracture.^{29–31} Scifer, as the wire is known, is made by drawing a dual phase microstructure of ferrite and martensite in steel with the composition of Fe–0.2C–0.8Si–1Mn (wt-%) in the form of 10 mm diameter rods, into strands which individually have a diameter of ~ 8 μ m. This amounts to a huge deformation with a true strain in excess of 9. The dislocation cell size in the material becomes ~ 10 –15 nm (Fig. 4a). This is where much of the strength of Scifer comes from.^{30,31} A similar stainless steel thread is also available commercially.³²

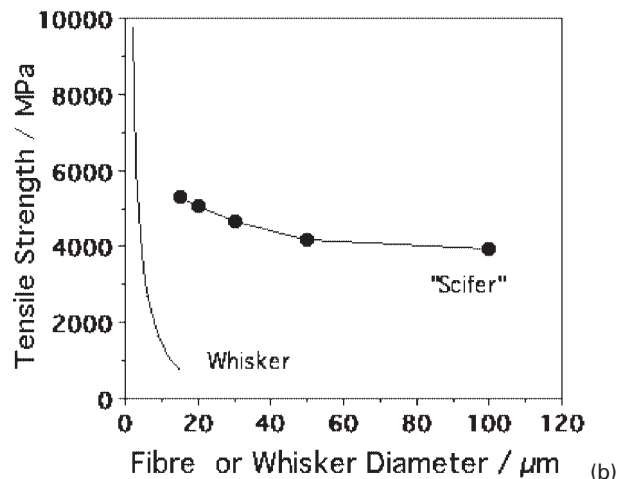
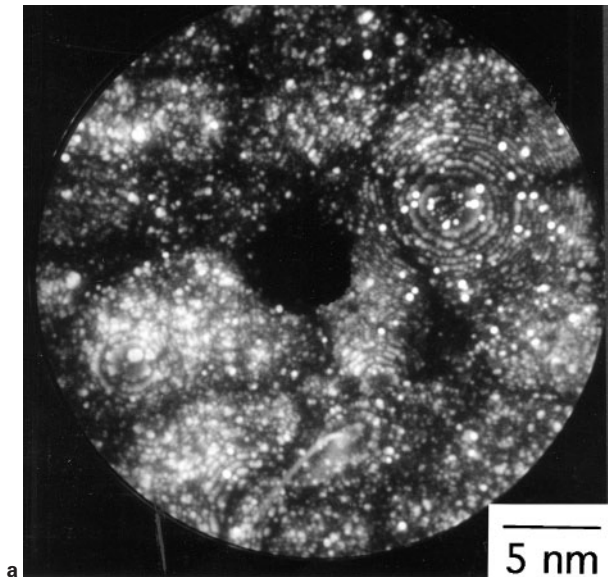
The fact that the properties are achieved by introducing defects also means that the strength of Scifer is insensitive to its size as shown in Fig. 4b.

A denier is the weight in grams of 9 km of fibre or yarn. A 50 denier thread is typically used in making socks whereas stockings are made from 10 denier fibre. Scifer is just 9 denier in this classification; this highlights one of the difficulties in using deformation to increase strength. The deformation necessary to accumulate a large number density of defects limits the size and form of the product, in the case of Scifer to that of a textile thread. Deformation processes, such as equichannel angular processing^{33,34} and accumulative roll bonding,^{35,36} maintain the overall dimensions, but the range of shapes that can be achieved is limited.

Statement 3: the properties of severely deformed materials are insensitive to size, but the forms that can be produced are limited.

Table 2 Stored energy and detonation or sound velocity

	Stored energy, J g ⁻¹	Detonation or sound velocity, m s ⁻¹
Dynamite	4650	6000
Carbon nanotube	5420	21 500



4 a Field ion microscope image of Scifer showing very fine dislocation cell structure,³¹ b comparison of size sensitivity of single crystal whiskers of iron and Scifer and c sock made using 50 denier yarn

Undeformed, fine polycrystalline steel

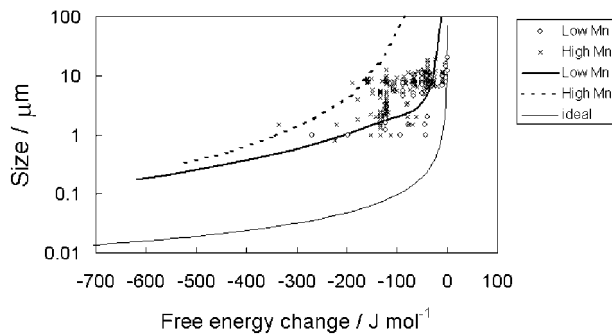
High strength low alloy steels, produced using thermo-mechanical processing, have been described as one of the wonders of the world.³⁷ The steels have contributed so much to the quality of engineered products that tens of billions of tonnes of such alloys now permeate all aspects of life. During the processing, fine austenite (γ) grains are generated by a combination of deformation and recrystallisation; the austenite finally transforms into fine grains of ferrite (α), typically with a size of 10 μm . The recent search has been for processes which reduce the grain size dramatically to <1 μm .³⁸⁻⁴⁰ Fine grains represent one of the few mechanisms available to

increase both strength and toughness. What then is the theoretical minimum grain size that can be achieved using this technology? This question can be answered by noting that the excess energy stored in the form of grain boundaries cannot exceed the free energy change $\Delta G_V^{1/2}$ owing to the transformation of the austenite.⁴¹

For an equiaxed polycrystalline grain structure, the grain boundary surface per unit volume S_V is related to the grain size \bar{L} (mean lineal intercept) by the equation $S_V = 2/\bar{L}$. Then the stored energy per unit volume due to the grain boundaries is

$$\Delta G_V = \sigma S_V = 2\sigma/\bar{L} \tag{3}$$

where σ is the energy per unit area of boundary. The



5 Plot of logarithm of ferrite grain size v. free energy change at Ar_3

limiting grain size is obtained by equating this stored energy to the driving force

$$|\Delta G_V^{\alpha/\gamma}| \geq \sigma_\alpha S_V^\alpha - \sigma_\gamma S_V^\gamma \quad (4)$$

For equiaxed austenite grains, it becomes

$$|\Delta G_V^{\alpha/\gamma}| \geq \frac{2\sigma_\alpha}{\bar{L}_\alpha} - \frac{2\sigma_\gamma}{\bar{L}_\gamma} \quad (5)$$

It follows that the smallest ferrite grain size can be achieved when all of $G_V^{\alpha/\gamma}$ is used up in creating α/α grain boundaries, so that

$$\bar{L}_\alpha^{\min} = \frac{2\sigma_\alpha}{|\Delta G_V^{\alpha/\gamma}| + 2\sigma_\gamma/\bar{L}_\gamma} \quad (6)$$

this relationship would have to be modified when the austenite is pancaked before transformation and there are other details such as crystallographic texture that need to be taken into account.⁴¹

Figure 5 shows the variation in the limiting ferrite grain size (\bar{L}_α^{\min}) as a function of ΔG_V , calculated using equation (5) with $\sigma_\alpha = 0.6 \text{ J m}^{-2}$; given the absence of data, the $2\sigma_\gamma/\bar{L}_\gamma$ term in equation (6) was set to zero. These calculations are presented as the 'ideal' curve in Fig. 5. The curve indicates that at large grain sizes, \bar{L}_α^{\min} is sensitive to ΔG_V and therefore to the undercooling below the equilibrium transformation temperature. However, reductions in grain size in the submicrometre range require huge values of ΔG_V , meaning that the transformations would have to be suppressed to large undercoolings to achieve fine grain size.

As shown in Fig. 5, the points are experimental data; in some cases it is assumed that the grain size quoted in the literature corresponds to the mean lineal intercept. The curves, marked low and high Mn, represent calculated values of \bar{L}_α^{\min} after allowing for recalescence.⁴¹ Also plotted on Fig. 5 are points corresponding to measured ferrite grain sizes from the low and high Mn steels as described in Ref. 41; it is evident that $\bar{L}_\alpha = \bar{L}_\alpha^{\min}$ except at the lowest undercoolings. The data indicate that in spite of tremendous efforts, the smallest ferrite grain size obtained commercially using thermomechanical processing is stuck at $\sim 1 \mu\text{m}$.

The reason for this is recalescence, which is the heating of the sample caused by release of the latent heat of transformation at a rate which is so high that it cannot easily be dissipated by diffusion. This rise in temperature owing to recalescence reduces the effective undercooling and therefore the driving force for transformation.⁴¹ It can be seen from Fig. 5 that the

recalescence corrected curves show better agreement with the experimental data, indicating that at large undercoolings, the achievement of fine grain size is limited by the need to dissipate enthalpy during rapid transformation.

Statement 4: to achieve submicrometre grain sizes, it is necessary to transform at large undercoolings. But the rate of transformation then increases, leading to recalescence, which defeats the objective. Therefore, large scale thermomechanical processing is limited by recalescence and it is unlikely to lead to grain sizes which are uniformly less than $\sim 1 \mu\text{m}$.

Martensite

Very strong martensitic steels with strength $>3 \text{ GPa}$ already exist.⁴² This kind of martensite is produced in fairly large steel samples by rapid cooling from the austenitic condition. However, the dimensions can be limited by the need to achieve a uniform microstructure, a fact implicit in the original concept of hardenability. To increase hardenability requires the addition of expensive alloying elements. The rapid cooling can lead to undesirable residual stresses,^{43,44} which can ruin critical components and have to be accounted for in component life assessments.

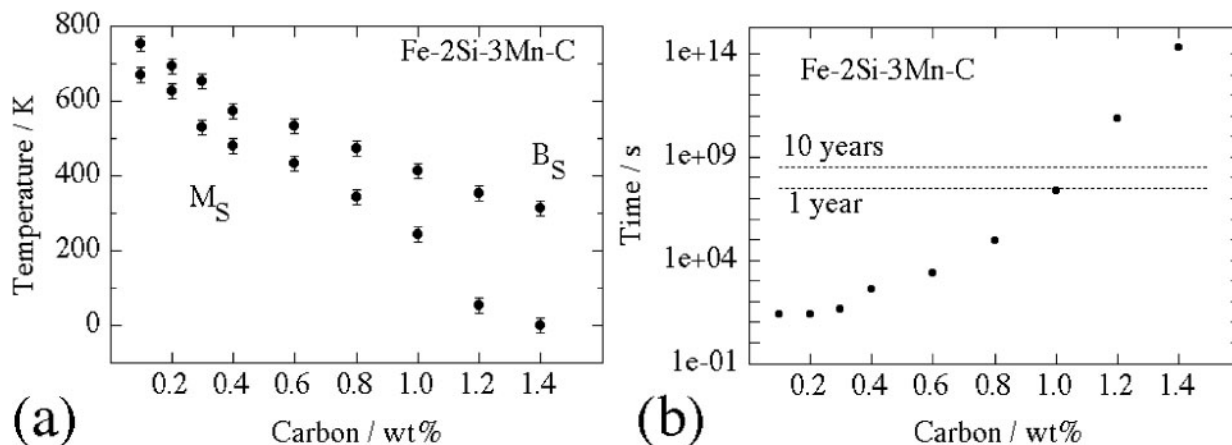
Design criteria

It would be nice to have a strong material which can be used for making components that are large in all their dimensions, and does not require mechanical processing or rapid cooling to reach the desired properties. To achieve this, the following conditions have been considered to be required:

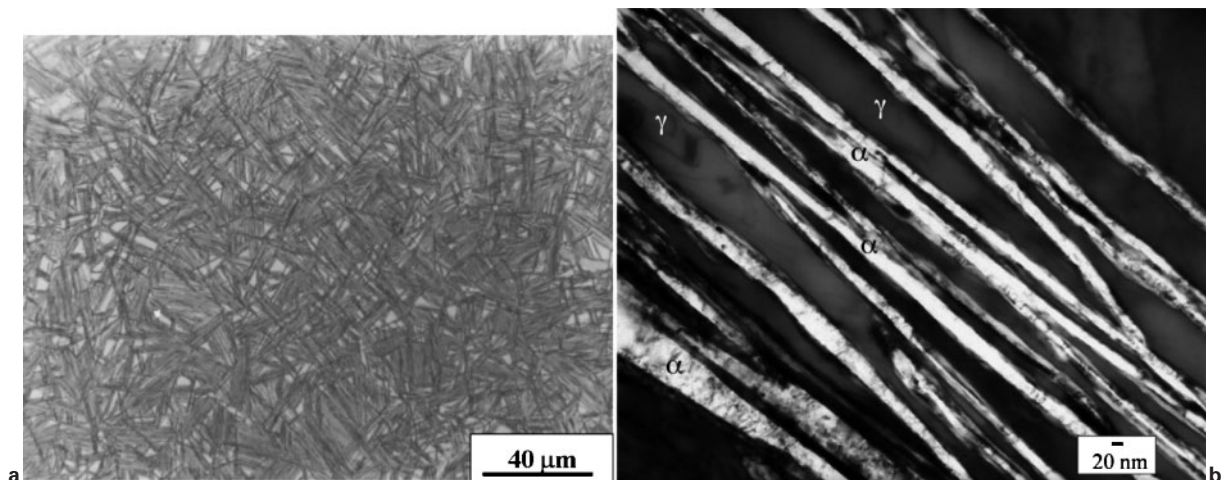
- (i) the material must not rely on perfection to achieve its properties. Strength can be generated by incorporating a large number density of defects such as grain boundaries and dislocations, but the defects must not be introduced by deformation if the shape of the material is not to be limited
- (ii) defects can be introduced by phase transformation. But to disperse them on a sufficiently fine scale, it requires the phase change to occur at large undercoolings (large free energy changes)
- (iii) a strong material must be able to fail in a safe manner. It should be tough
- (iv) recalescence limits the undercooling that can be achieved. Therefore, the product phase must be such that it has a small latent heat of formation and grows at a rate which allows the ready dissipation of heat.

Hard bainite

Steel transformed into carbide free bainite can satisfy these criteria. Bainite and martensite are generated from austenite without diffusion by a displacive mechanism. Not only does this lead to solute trapping but also a huge strain energy term, both of which reduce the heat of transformation.⁴⁵⁻⁴⁷ The growth of individual plates in both of the transformations is fast, but unlike martensite, the overall rate of the reaction is much



6 a Calculated transformation start temperatures in Fe-2Si-3Mn steel as function of carbon concentration and b Calculated time required to initiate bainite at B_S temperature⁵⁴



7 a optical micrograph; b transmission electron micrograph Fe-0.98C-1.46Si-1.89Mn-0.26Mo-1.26Cr-0.09V (wt-%) transformed at 200°C for 5 days^{56,58,59}

smaller for bainite. This is because the transformation propagates according to a subunit mechanism in which the rate is controlled by nucleation rather than by growth.⁴⁸ This mitigates recalescence.

Suppose we now attempt to calculate the lowest temperature at which bainite can be induced to grow. We have the theory to address this proposition.⁴⁹⁻⁵³ Such calculations are illustrated in Fig. 6a, which shows for an example steel, how the bainite start B_S and martensite start M_S temperatures vary as a function of the carbon concentration. In principle, there is no lower limit to the temperature at which bainite can be generated. On the other hand, the rate, at which bainite forms, slows down drastically as the transformation temperature is reduced (Fig. 6b). It may take hundreds or thousands of years to generate bainite at room temperature. For practical purposes, a transformation time of tens of days is reasonable. But why bother to produce bainite at a low temperature?

It is well known that the scale of the microstructure, i.e. the thickness of bainite plates, decreases as the transformation temperature is reduced.^{46,55} This is because the yield strength of the austenite becomes greater at lower temperatures, thereby affecting the plastic accommodation of the shape deformation accompanying bainite growth, and presumably because the nucleation rate can be greater at larger

undercoolings. The strength of the microstructure scales with the inverse of the plate thickness, thus providing a neat way of achieving strength without compromising toughness.

Experiments consistent with the calculations (Fig. 6) demonstrated that in a Fe-1.5Si-2Mn-1C (wt-%) steel (detailed composition in Table 3), bainite can be generated at a temperature as low as 125°C.⁵⁶ The temperature is so low that the diffusion distance of an iron atom is an inconceivable 10^{-17} m over the time scale of the experiment!

What is even more remarkable is that the plates of bainite are only 20–40 nm thick. The slender plates of

Table 3 Typical chemical compositions of hard bainite*

C	Si	Mn	Mo	Cr	V	Co	Al	Reference
0.98	1.46	1.89	0.26	1.26	0.09			56
0.83	1.57	1.98	0.24	1.02		1.54		61
0.78	1.49	1.95	0.24	0.97		1.60	0.99	61

*The silicon is added to prevent cementite formation during the growth of bainite, the molybdenum to counter embrittlement owing to impurities such as phosphorus, the manganese and chromium for hardenability and the cobalt and aluminum to accelerate the transformation. The substitutional solute also contributes to hardenability and determine the T_0 curve which is vital in the design of carbide free bainitic steels.^{62,63}

bainite are dispersed in stable carbon enriched austenite which, with its face centred cubic lattice, buffers the propagation of cracks. The optical and transmission electron microstructures are shown in Fig. 7; they not only have metallurgical significance in that they confirm calculations, but also are elegant to look at. Indeed, the microstructure has now been characterised both chemically and spatially to an atomic resolution; the pleasing aesthetic appearance is maintained at all resolutions. There is no redistribution of substitutional atoms on the conceivable finest scale.⁵⁷

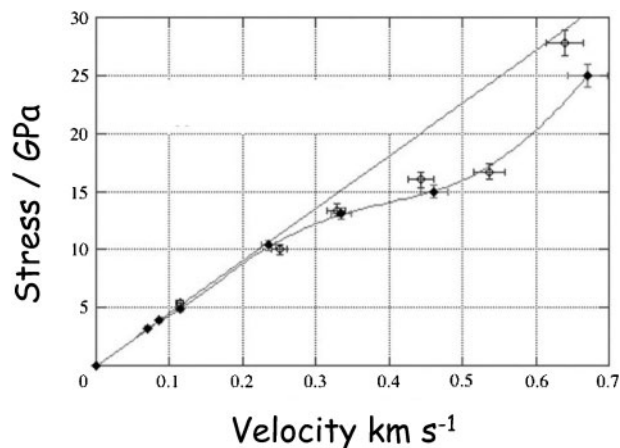
An ultimate tensile strength of 2500 MPa in tension has routinely been obtained, ductilities in the range 5–30% and toughness in excess of 30–40 MPa m^{1/2}. All this in a dirty steel that has been prepared ordinarily and hence contains inclusions and pores that would not be there when the steel is made by any respectable process. The bainite is also the hardest ever achieved, 700 HV.⁵⁶ The simple heat treatment involves the austenitisation of a chunk of steel (at say 950°C), followed by a gentle transfer into an oven at a low temperature (at say 200°C) and holding for ten days or so to generate the microstructure. There is no rapid cooling; residual stresses are avoided. The size of the specimen can be large because the time taken to reach 200°C from the austenitisation temperature is much less than that is required to initiate bainite. The tests performed by authors indicate uniform microstructure in 80 mm thick samples – thicker specimens were not available but calculations indicate that dimensions >200 mm will show similar results. This is a major commercial advantage.⁶⁰

It is cheap to heat treat something at temperatures where pizzas are normally cooked. But suppose that there is a need for a more rapid process. The transformation can easily be accelerated to occur within hours by adding solutes, which decrease the stability of austenite. Aluminium and cobalt, in concentrations <2 wt-%, have been shown to accelerate the transformation in the manner described. Both are effective, either on their own or in combination.⁶¹

Much of the strength and hardness of the microstructure comes from the very small thickness of the bainite plates. Of the total strength of 2500 MPa, ~1600 MPa can be attributed to the fineness of the plates. The residue of strength comes from dislocation forests, the strength of the iron lattice and the resistance to dislocation motion owing to solute atoms. Because there are many defects created during the growth of the bainite,⁴⁶ a large concentration of carbon remains trapped in the bainitic ferrite and does not precipitate probably because it is trapped at defects.⁶⁵

Strong bainite: armour

Whereas the ordinary tensile strength of the strong bainite is ~2.5 GPa, the strength has been reported to be as high as 10 GPa at the very high strain rates (10⁷ s⁻¹) associated with ballistic tests illustrated in Fig. 8.⁶⁶ Therefore, the strong bainite has found application in armour.^{67,68} Figure 9 shows a series of tests conducted using projectiles, which are said to involve ‘the more serious battlefield tests’ (the details are proprietary). Figures 9a and b show the experiments in which an armour system is tested. A 12 mm thick specimen of the bainitic steel is sandwiched between



8 Ballistic test on bainitic armour alloys.⁶⁶ Departure from straight line indicates plasticity and horizontal axis represents projectile velocity

vehicle steels, the whole contained in glass reinforced plastic. In ordinary armour, the projectile would have completely penetrated whereas the bainitic steel has prevented this; however, the steel did crack. Reducing the hardness (transforming at a higher temperature), it was possible for the armour to support multiple hits without being incorporated in an armour system (Fig. 9c).

The ballistic mass efficiency (BME) of an armour is defined as

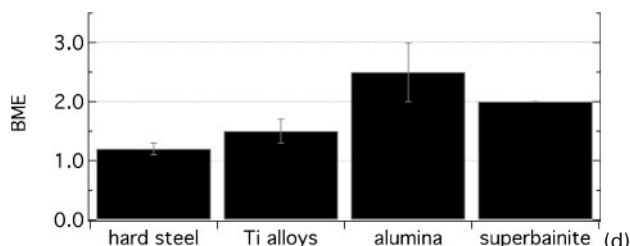
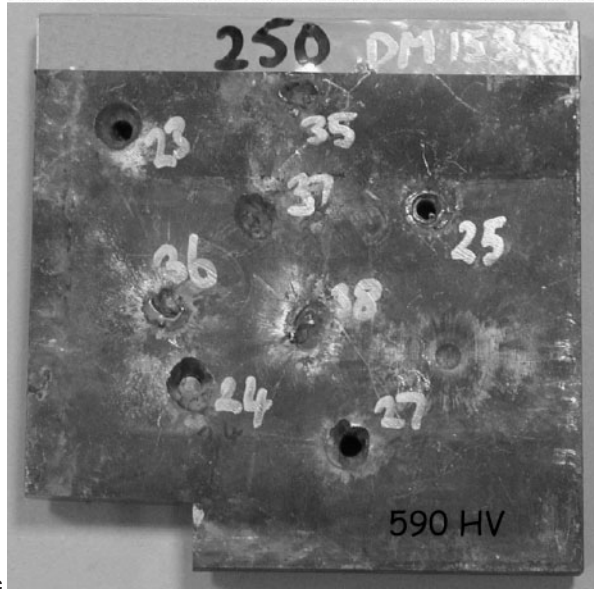
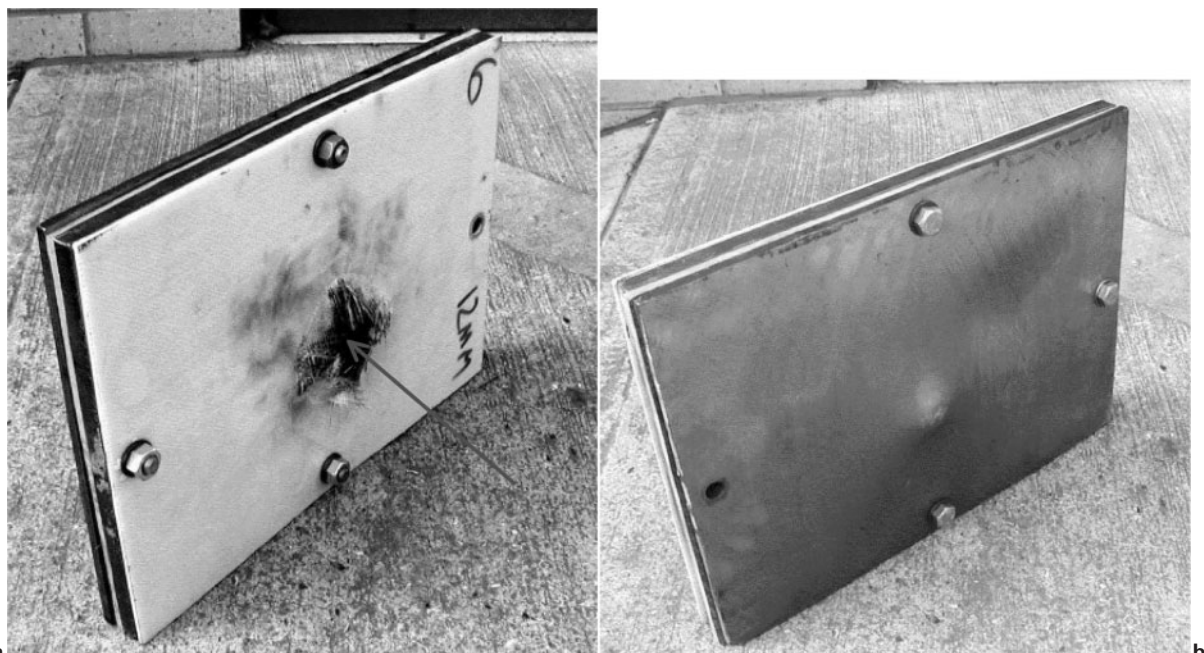
$$BME = \frac{\text{mass of ordinary armour to defeat a given threat}}{\text{mass of test armour to defeat same threat}} \quad (7)$$

Figure 9d shows that the BME of the strong bainite exceeds that of titanium armour and compares with that of alumina.⁶⁷

Low carbon hard bainite?

High carbon steels are difficult to weld because of the formation of untempered, brittle martensite in the coarse grained heat affected zones of the joints. The martensite fractures easily, leading to a gross deterioration in the structural integrity of the joint. For this reason, the vast majority of weldable steels have low carbon concentrations. Therefore, it would be desirable to make the low temperature bainite with a much reduced carbon concentration.

Calculations performed using the scheme outlined in Refs. 49 and 69, indicate that carbon is much more effective in maintaining a difference between the M_S and B_S temperatures than are substitutional solutes which reduce $|\Delta G^{*2}|$ simultaneously for martensite and bainite (Fig. 10). Substitutional solutes do not partition at any stage in the formation of martensite or bainite; therefore, both transformations are identically affected by the way in which the substitutional solute alters the thermodynamic driving force. It is the partitioning of carbon at the nucleation stage which is one of the distinguishing features of bainite when compared with martensite. This carbon partitioning allows bainite to form at a higher temperature than martensite. This advantage is diminished as the overall carbon concentration is reduced (Fig. 10).



a 12 mm thick specimen of bainite between two plates of ordinary vehicle armour with layer of glass reinforced plastic, arrow indicates path of projectile; b rear view showing lack of penetration; c lower hardness bainitic armour remaining intact following multiple hits; d comparison of armours

9 Fe-0.98C-1.46Si-1.89Mn-0.26Mo-1.26Cr-0.09V (wt-%) transformed at 200°C for 5 days⁶⁷

From these results, it must be concluded that it is impossible to design low temperature bainite with a low carbon concentration.

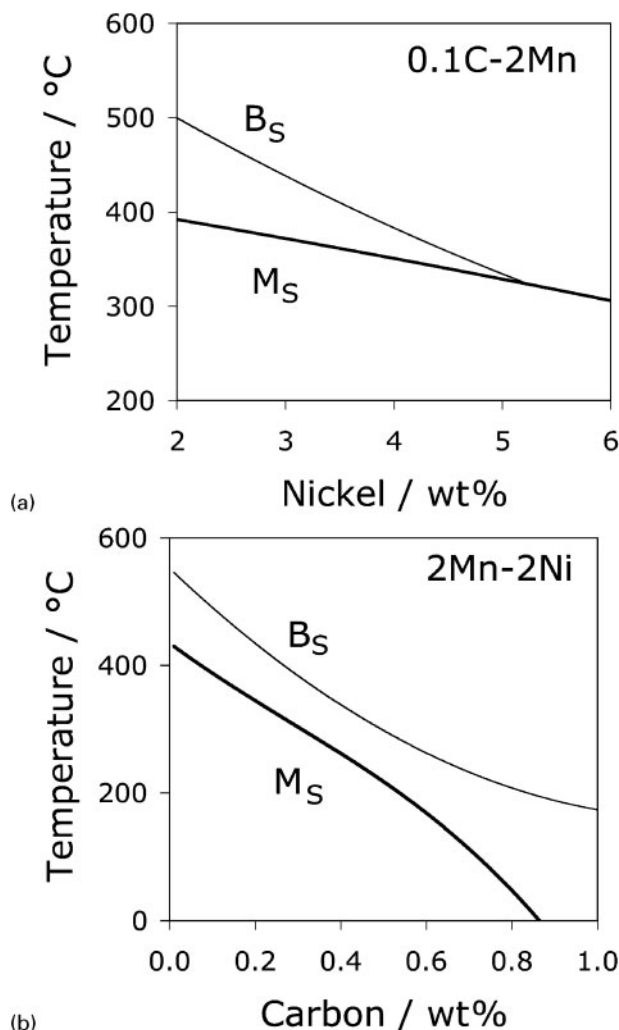
Summary

The ultimate focus of the lecture has been the ability to make large chunks of strong and tough steel. But it has been necessary to place this in the wider context of strong materials in order to allow sensible comparisons to be made.

When claims are made about strong materials for structural applications, they seem frequently to neglect the elementary science of scale. Just because it is possible to produce a carbon nanotube which has a calculated strength of 130 GPa and a measured strength approaching that value, it does not mean that this can be translated into a fibre of a length visible

to the naked eye, let alone the 120 000 km needed to begin thinking about a space elevator. Indeed, it may not be possible even in principle to scale the properties given the existence of entropy stabilised equilibrium defects.

In the contemporary materials literature, it is noticeable that strength is a much abused term. It is common to claim that a novel material is as strong as steel without specifying the nature of the steel against which the comparison is made. The claimants either ignore of the fact that it is possible to commercially make polycrystalline iron with a strength as low as 50 MPa or as high as 5.5 GPa, or neglect it to impress a fickle audience. In an academic context, single crystals of iron have been made which behave elastically to a stress of 14 GPa, taking them into a range of recoverable strain where Hooke's law does not apply.



(a) Fe-0.1C-2Mn with variation in nickel concentration; b Fe-2Ni-2Mn with variation in carbon concentration
 10 Calculated bainite and martensite start temperatures⁶⁹

Statement 5: the bainite, obtained by transformation at very low temperatures, is the hardest ever, has considerable ductility (almost all of it uniform), does not require mechanical processing, and does not require rapid cooling. Therefore, the steel after heat treatment does not have long range residual stresses. It is very cheap to produce and has uniform properties in very large sections. In effect, the hard bainite has achieved all of the essential objectives of structural nanomaterials which are the subject of so much research... BUT IN LARGE CHUNKS!

As is always the case, there remain many parameters that have yet to be characterised, for example the fatigue and stress corrosion properties.

Acknowledgements

The author is grateful to M. Endo for providing the images of the graphene and the schematic illustration of the graphene to nanotube transition. It is an especial pleasure to acknowledge Francisca Garcia Caballero for the original work on hard bainite. I would also like to thank Carlos Garcia Mateo, Mathew Peet, Kazu Hase,

Suresh Babu, Mike Miller, Peter Brown, David Crowther and others who continue to contribute to the subject.

References

- G. F. Taylor: *Phys. Rev.*, 1924, **23**, 655–660.
- C. Herring and J. K. Galt: *Phys. Rev.*, 1952, **85**, 1060–1062.
- G. W. Sears, A. Gatti and R. L. Fullman: *Acta Metall.*, 1954, **2**, 727–728.
- W. W. Piper and W. L. Roth: *Phys. Rev.*, 1953, **92**, 503.
- S. S. Brenner: *Acta Metall.*, 1956, **4**, 62–74.
- R. L. Eisner: *Acta Metall.*, 1955, **3**, 414–419.
- S. S. Brenner: *J Appl. Phys.*, 1956, **27**, 1484–1491.
- J. Frenkel: *Z. Phys.*, 1926, **37**, 572–609.
- A. H. Cottrell: *Eur. Rev.*, 1993, **1**, 169–176.
- G. R. Speich, A. J. Schwoeble and W. C. Leslie: *Metall. Trans.*, 1972, **3**, 2031–2037.
- B. C. Edwards: *Acta Astronaut.*, 2000, **47**, 735–744.
- D. V. Smitherman, Jr: 'An advanced earth-space infrastructure for the new millenium', Report NASA/CP-2000-210429, NASA Space Flight Centre, Huntsville, AL, 2000, 1–48.
- A. Oberlin, M. Endo and T. Koyama: *J. Cryst. Growth*, 1976, **32**, 335–349.
- H. W. Kroto, J. R. Heath, S. C. O'Brien, R. F. Curl and R. E. Smalley: *Nature*, 1985, **355**, 162–163.
- S. Iijima: *Nature*, 1991, **354**, 56–58.
- M. Endo, T. Hayashi, Y. A. Kim, M. Terrones and M. S. Dresselhaus: *Phil. Trans. R. Soc. Lond. A*, 2004, **362**, 2223–2238.
- H. Terrones, M. Terrones, F. López-Urías, J. A. Rodríguez-Manzo and A. L. Mackay: *Phil. Trans. R. Soc. Lond. A*, 2004, **362**, 2039–2063.
- M. S. Dresselhaus, G. Dresselhaus, J. C. Charlier and E. Hernández: *Phil. Trans. R. Soc. Lond. A*, 2004, **362**, 2065–2098.
- E. W. Wang, P. E. Sheehan and C. M. Lieber: *Science*, 1997, **277**, 1971–1975.
- J. P. Lu: *J. Phys. Chem. Solids*, 1997, **58**, 1649–1652.
- B. I. Yakobson and R. E. Smalley: *Am. Sci.*, 1997, **85**, 324–337.
- A. J. Stone and D. J. Wales: *Chem. Phys. Lett.*, 1986, **128**, 501.
- J. W. Christian: 'Theory of transformations in metals and alloys', Part I, 2nd edn; 1975, Oxford, Pergamon Press.
- S. L. Mielke, D. Troya, S. Zhang, J.-L. Li, S. Xiao, R. Car, R. S. Ruoff, G. C. Schatz and T. Belytschko: *Chem. Phys. Lett.*, 2004, **390**, 413–420.
- B. G. Demczyk, Y. M. Wang, J. Cumings, M. Hetman, W. Han, A. Zettl and R. O. Ritchie: *Mater. Sci. Eng. A*, 2002, **334A**, 173–178.
- M.-F. Yu, O. Lourie, M. J. Dyer, K. Moloni, T. F. Kelly and R. S. Ruoff: *Science*, 2000, **287**, 637–640.
- S. Xie, W. Li, Z. Pan, B. Chang and L. Sun: *J. Phys. Chem. Solids*, 2000, **61**, 1153–1158.
- Z. W. Pan, S. S. Xie, L. Lu, B. H. Chang, L. F. Sun, W. Y. Zhou, G. Wang and D. L. Zhang: *Appl. Phys. Lett.*, 1999, **74**, 3152–3154.
- Anonymous: 'Kobelco technology review No. 8', Kobe Steel Ltd, Japan, June 1990.
- H. K. D. H. Bhadeshia: in 'Future developments in metals and ceramics', (ed. J. A. Charles, G. W. Greenwood and G. C. Smith), 25–73; 1992, London, Institute of Materials.
- H. K. D. H. Bhadeshia and H. Harada: *Appl. Sur. Sci.*, 1993, **67**, 328–333.
- H.-S. Wang, J. R. Yang and H. K. D. H. Bhadeshia: *Mater. Sci. Technol.*, 2005, **21**, 1323–1328.
- R. Z. Valiev, R. K. Islamgaliev and I. V. Alexandrov: *Prog. Mater. Sci.*, 2000, **45**, 103–189.
- V. M. Segal: *Mater. Sci. Eng. A*, 2002, **338A**, 331–344.
- Y. Saito, N. Tsuji, H. Utsunomiya, T. Sakai and R. J. Hone: *Scripta Mater.*, 1998, **39**, 1221–1227.
- N. Tsuji, Y. Saito, H. Utsunomiya and S. Tanigawa: *Scripta Mater.*, 1999, **40**, 795–800.
- K. Easterling: 'Tomorrow's materials'; 1988, London, The Institute of Materials.
- D. P. Harvey, R. Kalyanaraman and T. S. Sudarshan: *Mater. Sci. Technol.*, 2002, **18**, 959–963.
- Z. Horita, M. Furukawa, M. Nemoto and T. G. Langdon: *Mater. Sci. Technol.*, 2000, **16**, 1239–1245.
- R. Priestner and A. K. Ibraheem: *Mater. Sci. Technol.*, 2000, **16**, 1267–1272.
- T. Yokota, C. Garcia-Mateo and H. K. D. H. Bhadeshia: *Scripta Mater.*, 2004, **51**, 767–770.

42. E. Hornbogen: Proc. 34th Sagamore Army Conf.: 'Innovations in ultrahigh-strength steel technology', (ed. G. B. Olson, M. Azrin and E. S. Wright), 113–126; 1987, Boston, MA, USA.
43. P. J. Withers and H. K. D. H. Bhadeshia: *Mater. Sci. Technol.*, 2001, **17**, 355–365.
44. P. J. Withers and H. K. D. H. Bhadeshia: *Mater. Sci. Technol.*, 2001, **17**, 366–375.
45. J. W. Christian: Proc. Int. Conf. ICOMAT '79 on 'Martensitic transformations', (ed. M. Cohen), 220–234; 1979, Boston, MA, MIT Press.
46. H. K. D. H. Bhadeshia: 'Bainite in steels', 2nd edn; 2002, London, IOM Communications.
47. H. K. D. H. Bhadeshia: *Mater. Sci. Forum*, 1998, **284–286**, 39–50.
48. H. Matsuda and H. K. D. H. Bhadeshia, *Proc. R. Soc. Lond. A*, 2004, **460**, 1710–1722.
49. H. K. D. H. Bhadeshia: *Acta Metall.*, 1981, **29**, 1117–1130.
50. H. K. D. H. Bhadeshia: *Met. Sci.*, 1981, **15**, 175–177.
51. H. K. D. H. Bhadeshia: *Met. Sci.*, 1981, **15**, 178–180.
52. G. Ghosh and G. B. Olson: *J. Phase Equilib.* 2001, **22**, 199–207.
53. C. G. Mateo and H. K. D. H. Bhadeshia: *Mater. Sci. Eng. A*, 2004, **378A**, 289–292.
54. H. K. D. H. Bhadeshia: *Met. Sci.*, 1982, **16**, 159–165.
55. S. B. Singh and H. K. D. H. Bhadeshia: *Mater. Sci. Eng. A*, 1998, **245A**, 72–78.
56. C. Garcia-Mateo, F. G. Caballero and H. K. D. H. Bhadeshia: *ISIJ Int.*, 2003, **43**, 1238–1243.
57. M. Peet, S. S. Babu, M. K. Miller and H. K. D. H. Bhadeshia: *Scripta Mater.*, 2004, **50**, 1277–1281.
58. F. G. Caballero, H. K. D. H. Bhadeshia, K. J. A. Mawella, D. G. Jones and P. Brown: *Mater. Sci. Technol.*, 2002, **18**, 279–284
59. C. Garcia-Mateo, F. G. Caballero and H. K. D. H. Bhadeshia: *J. Phys. Colloque*, 2003, **112**, 285–288
60. H. K. D. H. Bhadeshia: *Millenium Steel*, 2004, **5**, 25–28.
61. C. Garcia-Mateo, F. G. Caballero and H. K. D. H. Bhadeshia: *ISIJ Int.*, 2003, **43**, 1821–1825.
62. H. K. D. H. Bhadeshia and D. V. Edmonds: *Met. Sci.*, 1983, **17**, 411–419.
63. H. K. D. H. Bhadeshia and D. V. Edmonds: *Met. Sci.*, 1983, **17**, 420–425.
64. F.G. Caballero and H. K. D. H. Bhadeshia: *Curr. Opin. Solid State Mater. Sci.*, 2004, **8**, 251–257.
65. M. Peet, C. Garcia-Mateo, F. G. Caballero and H. K. D. H. Bhadeshia: *Mater. Sci. Technol.*, 2004, **20**, 814–818.
66. R. I. Hammond and W. G. Proud: *Proc. R. Soc. Lond. A*, 2004, **A460**, 2959–2974.
67. D. Crowther and P. M. Brown: Private communication, 2004.
68. P. M. Brown and D. P. Baxter: Proc. Conf. MS&T 2004, New Orleans, LA, USA, 2004, TMS/ASM, 433–438.
69. H. K. D. H. Bhadeshia: Proc. Int. Conf. Phase Transformations 2005, Warrendale, USA, TMS, 2005, to be published.
70. C. Garcia-Mateo, F. G. Caballero and H. K. D. H. Bhadeshia: *ISIJ Int.*, 2003, **43**, 1821–1825.